

Reionization, SLOAN, and WMAP: is the Picture Consistent?

Nickolay Y. Gnedin

Center for Astrophysics and Space Astronomy, University of Colorado, Boulder, CO 80309

gnedin@casa.colorado.edu

ABSTRACT

I show that advanced simulations of cosmological reionization are able to fit the observed data on the mean transmitted flux in the hydrogen Lyman-alpha line at $z \sim 6$. At the same time, posteriori models can be constructed that also produce a large value (20%) for the Thompson scattering optical depth, consistent with the WMAP measurements. Thus, it appears that a consistent picture emerges in which early reionization (as suggested by WMAP) is complete by $z \sim 6$ in accord with the SLOAN data.

Subject headings: cosmology: theory - cosmology: large-scale structure of universe - galaxies: formation - galaxies: intergalactic medium

1. Introduction

Are we knocking at the door of reionization? At least, it seems so, as the SLOAN quasar survey continues to find ever more distant quasars (Becker et al. 2001; Fan et al. 2002, 2003; White et al. 2003). In fact, highest redshift quasars show essentially no transmitted flux just blueward of the quasar HII region, which has been interpreted as the evidence that reionization took place at a redshift $z \sim 6$ (Becker et al. 2001; White et al. 2003; a similar claim was also made by Djorgovski et al. 2001 based on an extrapolation from a lower redshift observations).

However, one should be cautious before drawing such a conclusion. Indeed, the observed decrease in the mean transmitted flux at $z \sim 6$ might simply indicate a decrease in the mean ionizing intensity rather than a real reionization of the universe. After all, a neutral fraction of only 2×10^{-4} is sufficient to absorb effectively all Lyman-alpha radiation at $z = 6$ even in the gas that is underdense by a factor of 10. Thus, without an understanding of the evolution of the universe around the reionization epoch, the Ly-alpha absorption data cannot be used to constrain the epoch of reionization (unless damping wings are observed in the absorption profiles, Miralda-Escudé 1998).

Fortunately, our theoretical understanding of

the process of reionization, in part based on numerical simulations, is solid enough so that the evolution of the ionizing intensity at these redshifts can be predicted with a reasonable confidence level. Combining simulations with the observational data indeed allows one to come up with a consistent picture for the process of cosmological reionization.

2. Simulations

Four sets of simulations have been performed with the SLH code and are similar to the simulations reported in Gnedin (2000). The main difference with previous simulations is that a newly developed and highly accurate Optically Thin Eddington Variable Tensor (OTVET) approximation for modeling radiative transfer (Gnedin & Abel 2001) is used instead of a crude Local Optical Depth approximation. The new simulations therefore should be sufficiently accurate (subject to the usual limitations of numerical convergence and phenomenological description of star formation) to be used meaningfully in comparing with the observational data. In particular, my fiducial model used the cosmological parameters as determined by the *WMAP* satellite (Spergel, et al. 2003).

Parameters of the four sets are given in Table 1. All simulations included 128^3 dark matter parti-

cles, an equal number of baryonic cells on a quasi-Lagrangian moving mesh, and about 3 million stellar particles that formed continuously during the simulation. The nominal spatial resolution of simulations with the box size of $4h^{-1}$ Mpc was fixed at $1h^{-1}$ comoving kpc, with the real resolution being a factor of two worse. Simulations with the box size of $8h^{-1}$ Mpc had the twice worse spatial resolution.

In all cases a flat cosmology was assumed, with $\Omega_{\Lambda,0} = 1 - \Omega_{m,0}$, and normalization of the primordial fluctuations was determined either from the *WMAP* data (Spergel et al. 2003) for sets A4 and A8, or from the *COBE* data (White & Bunn 1995). Notice that a small change in the slope of the primordial power-law spectrum n makes a significant effect on the amount of the small-scale power due to a large leverage arm from CMB scales to the tens-of-kpc scales which are important for reionization.

Star formation is incorporated in the simulations using a phenomenological Schmidt law, which introduces two free parameters: the star formation efficiency ϵ_{SF} (as defined by eq. (1) of Gnedin 2000) and the ionizing radiation efficiency ϵ_{UV} (defined as the energy in ionizing photons per unit of the rest energy of stellar particles).

The star formation efficiency ϵ_{SF} is chosen so as to normalize the global star formation rate in the simulation at $z = 4$ to the observed value from Steidel et al. (2001), whereas the ultraviolet radiation efficiency ϵ_{UV} is only weakly constrained by the (highly uncertain) mean photoionization rate at $z \sim 4$. The redshift of reionization strongly depends on ϵ_{UV} and is not in fact predicted in a simulation, but can be changed over a reasonable range depending on the assumed value of ϵ_{UV} . Each of the simulations sets included in Table 1 in fact included several individual simulations with different values of ϵ_{UV} .

However, since the simulations are quite expen-

Table 1: Simulation Parameters

Set	Ω_m	h	n	Box size (h^{-1} Mpc)
A4	0.27	0.71	1.0	4
A8	0.27	0.71	1.0	8
B4	0.35	0.70	0.95	4
C4	0.35	0.70	0.97	4

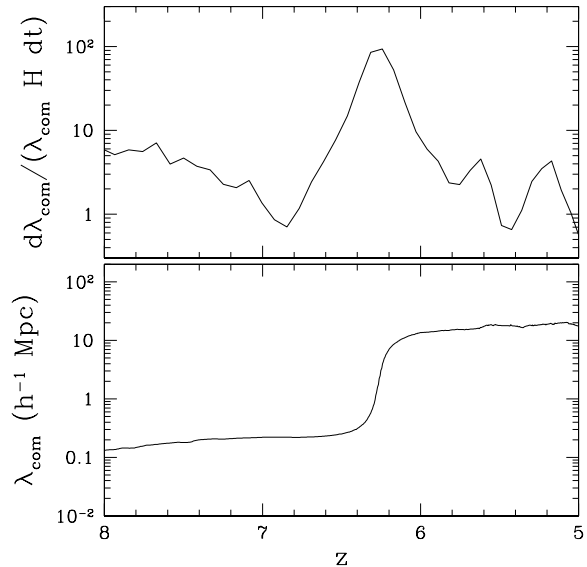


Fig. 1.— Mean free path to ionizing radiation (bottom) and its time derivative (top) as a function of redshift for the simulation A4 from Table 1.

sive, it is not possible to cover a large range of ϵ_{UV} in a given set. Typically, only 2 or 3 simulations per set have been performed and the results are then interpolated between the simulations. This procedure is fully described in §4.

3. A “Redshift of Reionization”: What Is It?

Reionization is a process, not an event. In fact, whole process of reionization is quite extended ($\Delta z \sim 5 - 10$), and can be generically separated into three stages: (i) the **pre-overlap stage**, in which individual HII regions around the sources of ionization expand and merge in the low density IGM, (ii) the **overlap stage**, in which all individual HII regions overlap, and last remnants of the neutral low density gas quickly disappear, and (iii) the **post-overlap stage**, in which remaining high density gas is being ionized from the outside, until neutral gas remains only in some of the highest density regions, which would be identified as Lyman-limit system in the absorption spectra of distant quasars.

One can think reionization as complete, when the mean free path to the ionizing radiation is fully

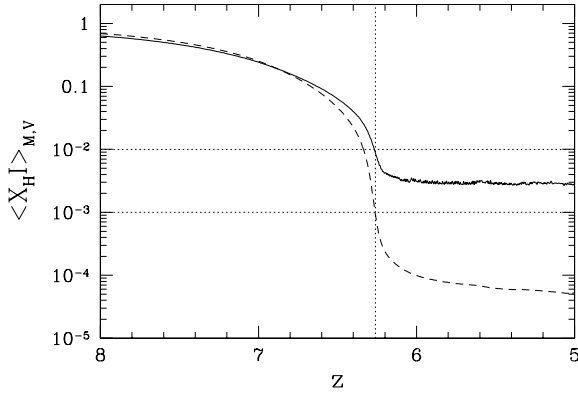


Fig. 2.— Mass (solid line) and volume (dashed line) weighted neutral hydrogen fraction as a function of redshift for the simulation A4 from Table 1. Notice that the peak in the time derivative of the mean free path (vertical dashed line) closely corresponds to the moment when the mean mass (volume) weighted neutral fraction reaches a value of 10^{-2} (10^{-3}) respectively.

determined by (relatively) slowly evolving Lyman-limit systems (Miralda-Escudé 2003a).

It is, however, tempting to try to assign a value for the “redshift of reionization”. Such a value, in order not to be completely arbitrary, must be related to the physics of the reionization process. For example, it seems to be natural to identify the moment of reionization with the overlap stage, but even it takes place over a sizable redshift interval $\Delta z \sim 1$ (Gnedin 2000), so we would need a better definition if we are to assign a value to “the redshift of reionization”.

Fortunately, such a definition exists. Figure 1 shows the mean free path to ionizing radiation and its time derivative as a function of redshift for the fiducial simulation (A4) with $\epsilon_{UV} = 1 \times 10^{-6}$. The time derivative of the mean free path has a well-defined peak in the middle of the overlap stage, which is a natural moment to identify with “the redshift of reionization” z_{REI} .

However, this definition is not entirely practical, since the time derivative of the mean free path cannot be observed directly. Instead, a more easily observable quantity is the mean neutral fraction. Figure 2 shows the mean mass and volume weighted neutral hydrogen fraction for the fiducial

simulation. The moment of reionization closely corresponds to the time when the mean mass (volume) weighted neutral fraction reaches a value of 10^{-2} (10^{-3}) respectively - one can consider that moment as an alternative definition to “the redshift of reionization”.

The latter definition is more practical, but it is a subject to an important clause: while the volume weighted neutral fraction is reliably computed in the simulation, the mass weighted one depends on the numerical resolution. In particular, the simulations presented in this paper do not resolve the damped Lyman-alpha systems, so the quoted above value of 1% for the mass weighted neutral fraction does not include the neutral gas locked in the damped Lyman-alpha systems. In this respect, the volume weighted number is more robust and should be used as a main definition of “the redshift of reionization”.

4. Results

4.1. Fitting the Mean Transmitted Flux Data

Figure 3 shows the mean transmitted flux as a function of redshift for the three simulations with different values of the ϵ_{UV} parameter from the set B4. The observational data shows with open circles were obtained from White et al. (2003) by averaging the mean transmitted flux at a given redshift interval. The vertical error-bars are errors of the mean (not mean errors!). The horizontal error-bars are simply the width of the redshift interval over which the mean transmitted flux is computed. The last data point (without the vertical error-bar) is likely to be contaminated by a foreground galaxy and is not included in this analysis. Filled squares show the data from Songaila (2004). In the latter case I do not show the error-bars for clarity, but they are comparable to that of White et al. (2003).

Two gray lines are the solid black line simply shifted horizontally. As one can see, the change in the ϵ_{UV} parameter simply translates into the shift in redshift. This is not surprising given that in the Λ CDM model clustering proceeds hierarchically, in a quasi self similar manner. In other words, one would expect that the dependence of the mean transmitted flux on the emissivity parameter ϵ_{UV}

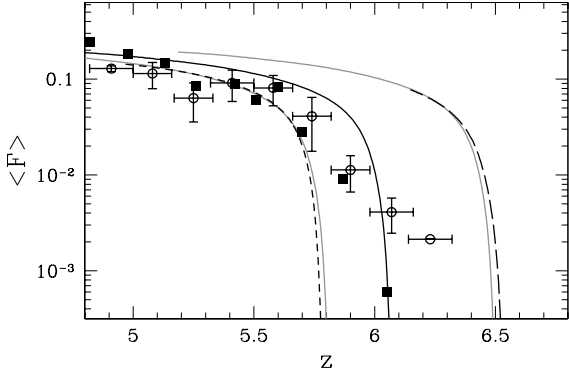


Fig. 3.— Mean transmitted flux as a function of redshift for simulations from the set B4. Solid, long-dashed, and short-dashed black lines correspond to simulations with $\epsilon_{UV} = 2.5 \times 10^{-6}$, 4.0×10^{-6} , and 2.0×10^{-6} respectively. Two gray lines are the solid black line simply shifted horizontally to match other two lines. Open circles with error-bars show the observational data from White et al. (2003) and filled squares are the data of Songaila (2004; the error-bars are not shown for these points for clarity).

and redshift z enters, to the first order, only as

$$\langle F \rangle(z) = (1+z)^\beta g[\epsilon_{UV}(1+z)^{-\alpha}], \quad (1)$$

where g is a function of one argument, and α and β depend on the slope of the primordial power spectrum at the scale of interest, and may also depend on the details of the temperature-density relation. But because I am only concerned with a narrow redshift range around $z = 6$ (for example, $z = 5.8 \div 6.5$ in Fig. 3), α and β from equation (1) can be considered constant in the first approximation. Fig. 3 indicates that for the range of redshifts considered β is small, less than about 0.5 in the absolute value. The specific reason for such a small value is not entirely clear, and may be a simple coincidence: if ϵ_{UV} is reduced, the amount of ionizing radiation in the post-overlap stage is also reduced, but at the same time the post-overlap stage is delayed to lower redshifts, when densities are lower. The two effects appear to approximately cancel each other, leading to a small value of β .

The main result of Fig. 3 is that a change in the emissivity parameter ϵ_{UV} by a factor of f simply translates into a rescale of (one plus) redshift by

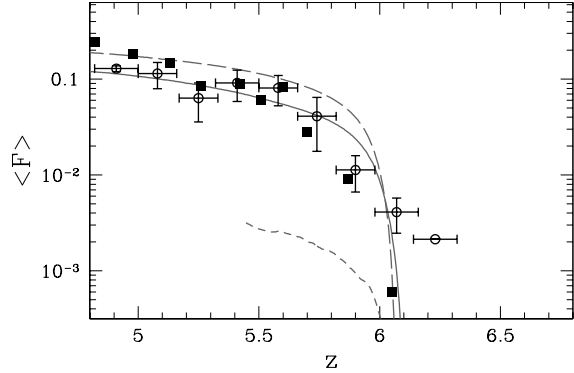


Fig. 4.— Mean transmitted flux as a function of redshift for best-fit simulations from sets A4 (solid line), B4 (long-dashed line), and C4 (short-dashed line).

a factor $f^{1/\alpha}$. Note that such rescaling does not affect the vertical amplitude of the mean transmitted flux curve. As is well known, the mean absorption after the post-overlap stage is dominated by the Lyman-limit systems (Miralda-Escudé 2003b). Thus, in order to reproduce the observed run of the mean transmitted flux with redshift, a simulation must have (i) the right value for the emissivity parameter ϵ_{UV} (i.e. the right value for the redshift of reionization), to reproduce the drop-off at $z \sim 6$, and (ii) the correct abundance of the Lyman-limit systems. The latter is crucially dependent on the abundance of low mass virialized objects, and is *not* completely controlled by the parameter ϵ_{UV} , but also depends on the mass function of virialized objects, i.e. on cosmological parameters. Therefore, if a simulation has wrong values of cosmological parameters, it might not be able to reproduce the amplitude of the mean transmitted flux as a function of redshift for *any* value of the single free parameter ϵ_{UV} .

This is illustrated in Figure 4 which shows the results from three simulation sets (A4, B4, and C4), each rescaled for the best value of the emissivity parameter ϵ_{UV} (the simulation set C4 has not been continued beyond $z = 5.5$). As one can see, not all of the simulation sets are able to reproduce the amplitude of the mean transmitted flux curve. For example, the set C4 predicts a factor of 10 more absorption: in that cosmologi-

cal model ($\Omega_m = 0.35$, $n = 0.97$) the amount of small-scale power is significantly larger than, say, in the *WMAP* model, and the mean distance between Lyman-limit systems is a factor of 10 less than the observed value. Sets A4 and B4, on the other hand, provide a reasonable, although not perfect, fit to the data. In fact, it appears that the set A4 (the *WMAP* model) fits the data best for $z > 5.2$, but goes somewhat below the data points at lower redshifts. This is expected, since due to the limited size of the computational box, simulations should underpredict the abundance of ionizing sources at lower redshifts. The simulation set B4 has a somewhat higher mean transmitted flux, although it is marginally consistent with the data given the cosmic variance.

There is no easy way to reconcile model C4 (and, perhaps, model B4) with the data. The abundance of the Lyman-limit systems depends not only on ϵ_{UV} , but also on the cosmological model, and, as long as ϵ_{UV} and cosmological parameters are specified, there is no free parameter left to adjust this abundance. The only way to make, say, model B4 to fit the data better would be to include additional Lyman-limit absorption posteriori, by hand - for example, by postulating an entirely different class of objects that contribute to the mean free path but do not form within the hierarchical clustering framework. For model C4, however, one would have to postulate that some of the Lyman-limit system that form in the simulation do not form in reality.

4.2. Measuring the Redshift of Reionization

Using the fact that the *WMAP* model fits the observed data, one can determine how much the redshift of reionization can be shifted while still preserving the acceptable fit to the data. Figure 5 shows the range of values for the redshift of reionization for models A4 and B4 (although the latter is admittedly a worse fit to the data) obtained by adding linearly two different components: (i) an average observational error-bar in z -direction (0.085), and (ii) the average uncertainty to the best fit value of z_{REI} for the fiducial model. With these three uncertainties included, a measurement of the redshift of reionization can be made:

$$z_{\text{REI}} = 6.1 \pm 0.3 \quad (95\% \text{ CL}). \quad (2)$$

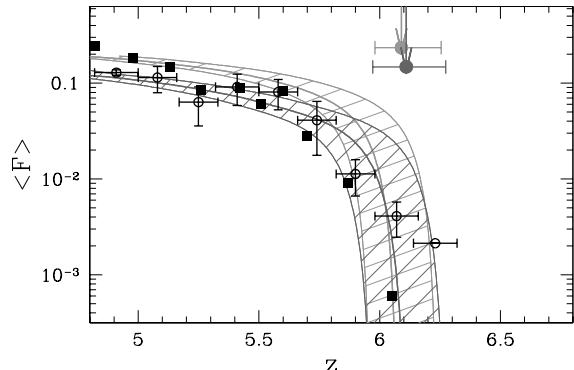


Fig. 5.— Mean transmitted flux as a function of redshift for the best-fit simulations from sets A4 (dark gray) and B4 (medium gray). Shaded regions illustrate the uncertainty due to observational errors. Arrows with error-bars give the redshift of reionization plus its 1σ uncertainty for each of the simulation sets.

If other cosmological models are also considered (for example, model B4), then an additional “systematic” uncertainty is introduced due to small differences in the redshifts of reionization of different cosmological models. This uncertainty, however, is rather small, as can be seen from Fig. 5, and is ignored here.

4.3. Sanity Checks

Before I can proceed further, several sanity tests must be completed. The first two are shown in Figure 6. The light gray line is again the best-fit fiducial *WMAP* model, with error-bars showing the rms fluctuation in the mean transmitted flux (error of the mean) - this is consistent with (although slightly smaller than) the observed values. This is not surprising, as a finite (and relatively small) size of the computational volume will lead to an underestimate of the cosmic variance.

How significant this overestimate? In order to reduce the cosmic variance at the box size scale, the specific realizations of initial conditions are selected to reproduce the correct power spectrum of initial perturbations on the fundamental mode (Gnedin & Hamilton 2002), which mitigates the uncertainty due to cosmic variance by about a factor of 10 or more. To demonstrate that numerical

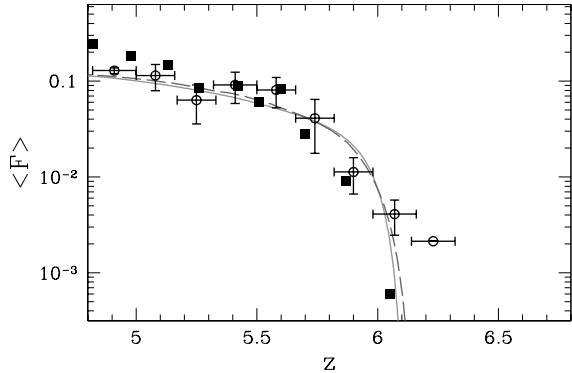


Fig. 6.— Tests of numerical convergence and cosmic variance. Light gray line with error-bars is the best fit A4 set with the expected rms fluctuation in the mean transmitted flux over a redshift interval $\Delta z = 0.17$ (which is the the average redshift interval over which the transmitted flux is averaged in the observational data). The dark gray long-dashed line is the best-fit mean transmitted flux for the A8 set (twice larger simulation volume).

convergence is achieved for the mean transmitted flux, and that cosmic variance does not affect my results, I show with the dark gray line in Fig. 6 the best-fit simulation from the A8 set (the same cosmological model, twice larger box). The fact that the two simulations with the two box sizes are sufficiently close argues for the numerical convergence of the simulation result, although, admittedly, this is not a 100% rigorous test (three different resolutions would be required for a complete test, but this is currently beyond the existing computer capabilities).

The recent results from the WMAP measurement of the cross-correlation between the temperature and polarization anisotropies of the CMB indicate the large value of the Compton optical depth $\tau = 0.12 \pm 0.06$ (Kogut et al. 2003, Tegmark et al. 2004). Does this observation rule out reionization at $z \sim 6$? Figure 7 shows the ionization histories for the fiducial model (which has $\tau = 0.06$) together with three other posteriori ionization histories which all have $\tau = 0.2$. Because these histories are adjusted to match the fiducial model before the volume averaged ionized fraction approaches 99.9%, they all have identical redshifts

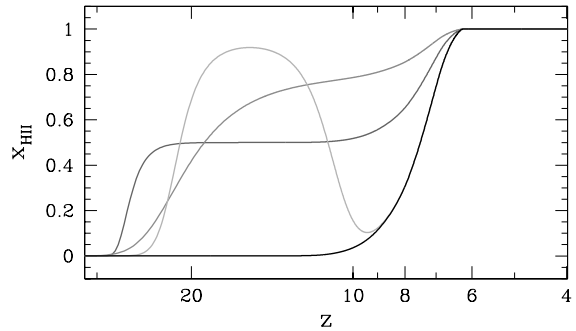


Fig. 7.— Ionization histories (volume averaged ionized fraction as a function of redshift) for the fiducial model (black line), and three arbitrary ionization histories (grey lines) with $\tau = 0.2$. All four model have the identical ionization redshift of $z_{\text{REI}} = 6.1$.

of reionization and identical mean transmitted flux curves at $z < 6.1$. Thus, the WMAP measurement by itself neither constraints the redshift of reionization nor contradicts the SLOAN data, but rather indicates that the early ionization history might have been quite complex.

5. Conclusions

I have shown that advanced self-consistent cosmological simulation with radiative transfer are able to reproduce the observed data on the evolution of the mean transmitted flux from the SLOAN survey when the values of cosmological parameters that best fit the WMAP data are adopted for the underlying cosmology. Thus, a consistent picture is emerging in which the universe reionizes at 6.1 ± 0.3 after possibly a prolonged period of partial reionization.

I am grateful to the anonymous referee for correcting errors in the original manuscript, and for other valuable comments. This work was supported by NSF grant AST-0134373 and by National Computational Science Alliance under grant AST-020018N and utilized SGI Origin 2000 array and IBM P690 array at the National Center for Supercomputing Applications.

REFERENCES

- Becker, R. H., et al. 2001, *AJ*, 122, 2850
- Djorgovski, S. G., Castro, S. M., Stern, D., Mahabal, A. 2001, *ApJL*, 560, 5
- Fan, X., et al. 2003, *AJ*, 125, 1649
- Fan, X., Narayanan, V. K., Strauss, M. A., White, R. L., Becker, R. H., Pentericci, L., & Rix, H.-W. 2002, *AJ*, 123, 1247
- Gnedin, N. Y. 2000, *ApJ*, 535, 530
- Gnedin, N. Y., Abel, T. 2001, *NewA*, 6, 437
- Gnedin, N. Y., Hamilton, A. J. S. 2002, *MNRAS*, 334, 107
- Kogut, A., et al. 2003, *ApJS*, 148, 161
- Miralda-Escudé, J. 1998, *ApJ*, 501, 15
- Miralda-Escudé, J. 2003a, *Science*, 300, 1904
- Miralda-Escudé, J. 2003b, *ApJ*, in press (astro-ph/0211071)
- Songaila, A. 2004, astro-ph/0402347
- Spergel, D. N., et al. 2003, *ApJ*, in press (astro-ph/0302209)
- Steidel, C. C., Adelberger, K. L., Ciavalisco, M., Dickinson, M., Pettini, M. 1999, *ApJ*, 519, 1
- Tegmark, M., et al. 2004, *ApJ*, submitted (astro-ph/0310723)
- White, M., & Bunn, E. F. 1995, *ApJ*, 450, 477
- White, R. L., Becker, R. H., Fan, X., & Strauss, M. A. 2003, *AJ*, 126, 1